ELSEVIER

Toxicon 50 (2007) 553–562

TOXICON

www.elsevier.com/locate/toxicon

Crotamine inhibits preferentially fast-twitching muscles but is inactive on sodium channels ☆

Carina T. Rizzi[a,d], João Luís Carvalho-de-Souza[b], Emanuele Schiavon[c], Antônio Carlos Cassola[b], Enzo Wanke[c], Lanfranco R.P. Troncone[a,*]

[a]*Laboratory of Pharmacology, Instituto Butantan, Av. Vital Brasil 1500, Sao Paulo SP-05503-900, Brazil*
[b]*Department of Pharmacology and Physiology, Institute of Biomedical Sciences, University of São Paulo, Brazil*
[c]*Department of Biotechnology and Biosciences, Laboratory of Neurophysiology, University of Milano, Bicocca, 20126 Milano, Italy*
[d]*Department of Physiology, Biosciences Institute, University of São Paulo, Brazil*

Received 15 March 2007; received in revised form 27 April 2007; accepted 30 April 2007
Available online 18 May 2007

Abstract

Crotamine is a peptide toxin from the venom of the rattlesnake *Crotalus durissus terrificus* that induces a typical hind-limb paralysis of unknown nature. Hind limbs have a predominance of fast-twitching muscles that bear a higher density of sodium channels believed until now to be the primary target of crotamine. Hypothetically, this makes these muscles more sensitive to crotamine and would explain such hind-limb paralysis. To challenge this hypothesis, we performed concentration vs. response curves on fast (extensor digitorum longus (EDL)) and slow (soleus) muscles of adult male rats. Crotamine was tested on various human Na^+ channel isoforms ($Na_v1.1$–$Na_v1.6$ α-subunits) expressed in HEK293 cells in patch-clamp experiments, as well as in acutely dissociated dorsal root ganglion (DRG) neurons. Also, the behavioral effects of crotamine intoxication were compared with those of a muscle-selective sodium channel antagonist μ-CgTx-GIIIA, and other sodium-acting toxins such as tetrodotoxin α- and β-pompilidotoxins, sea anemone toxin BcIII, spider toxin Tx2-6. Results pointed out that EDL was more susceptible to crotamine than soleus under direct electrical stimulation. Surprisingly, electrophysiological experiments in human $Na_v1.1$ to $Na_v1.6$ Na^+ channels failed to show any significant change in channel characteristics, in a clear contrast with former studies. DRG neurons did not respond to crotamine. The behavioral effects of the toxins were described in detail and showed remarkable differences. We conclude that, although differences in the physiology of fast and slow muscles may cause the typical crotamine syndrome, sodium channels are not the primary target of crotamine and therefore, the real mechanism of action of this toxin is still unknown.
© 2007 Elsevier Ltd. All rights reserved.

Keywords: *Crotalus durissus terrificus*; Crotamine; Sodium channels; Toxin; Behavior; Muscle

1. Introduction

Crotamine is a small basic peptide of 42 amino acids and 3 disulfide bonds, considered to be a myotoxin by several authors. Its three-dimensional structure has been proposed and several similarities with other small peptide toxins were described

☆ *Ethical statement*: We hereby certify that the Commission for the ethical use of animals in experimentation—Instituto Butantan has evaluated the experimental protocol entitled "Crotamine-induced hind limb paralysis—what is behind it?" and found it in accordance with the principles adopted by the Brazilian College of Animal Experimentation and registered under the authorization number 283/06.

*Corresponding author.
E-mail address: ltroncone@butantan.gov.br (L.R.P. Troncone).

0041-0101/$ - see front matter © 2007 Elsevier Ltd. All rights reserved.
doi:10.1016/j.toxicon.2007.04.026

(Beltran et al., 1985, 1990; Endo et al., 1989; Hampe et al., 1978; Laure, 1975; Nicastro et al., 2003). The most remarkable sign of crotamine intoxication in rodents is the typical hind-limb paralysis characterized by an extended posture with the hind limbs completely immobilized, resembling the effects of a medullar transaction (Cheymol et al., 1971; Teno et al., 1990). Some authors proposed that crotamine might act through changes in voltage-gated sodium channels (Chang and Tseng, 1978; Matavel et al., 1998). In an attempt to explain the crotamine's typical behavioral syndrome, we proposed a working hypothesis based on the fact that rodents have a clear predominance of fast-twitching muscles in the hind limbs that bear a much larger number of sodium channels than slow-twitching fibers (Bewick et al., 2004; Wang and Kernell, 2001a). This implies that fast-twitching fibers rely heavily on functional sodium channels and therefore would be more susceptible to sodium channel toxins than slow-twitching muscles. The rat slow-twitching muscle soleus, and the fast-twitching muscle extensor digitorum longus (EDL) were tested for crotamine blockade and the results partially support this hypothesis. This observation prompted us to evaluate whether crotamine has any preference for the muscle-type sodium channel, further supporting our hypothesis. The selectivity of crotamine for the different isoforms of voltage-dependent sodium channels was assayed in a whole-cell voltage clamp using transfected HEK cells expressing selectively human $Na_v1.1$–6 channels. The toxin was also assayed on dorsal root ganglion (DRG) cells in order to have a typical neuron expressing all the ancillary molecular machinery of sodium channels. Finally, the behavioral syndrome induced by crotamine was compared with those induced by injections of the prototypical muscle-selective sodium channel blocker μ-conotoxin-GIIIa, the classical blocker tetrodotoxin, the wasp toxins α- and β-pompilidotoxin, the sea anemone toxin BcIII, and the *Phoneutria nigriventer* toxin Tx2-6 known to delay sodium channel inactivation, in order to establish a pattern of behavioral signs that could mirror the action of this class of toxin and shed some light on the effects of crotamine.

2. Methods

2.1. Toxin purification

Crotamine has been purified and kindly supplied by Dr. P. Spencer from the Instituto de Pesquisas Energéticas e Nucleares (IPEN) at São Paulo. Purification was performed as described (Boni-Mitake et al., 2001), with the following modifications: 150 mg of crude lyophilized *Crotalus durissus terrificus* venom was dissolved in 2 ml of ammonium formiate buffer (100 mM, pH 3.0) and centrifuged at 200*g* for 10 min. The supernatant was then applied to a Superdex 75 gel filtration column previously equilibrated with the same buffer. Elution was monitored by UV detection at 280 nm and collected with an automatic fraction collector. Fractions with the main peaks were pooled and freeze-dried under vacuum. The crotamine fraction was dissolved in phosphate buffer 50 mM, pH 7.8, and applied to a Resource S FPLC column and eluted by a gradient of NaCl from 0 to 2 M. Elution was monitored by automatic UV detection at 280 nm, followed by dialysis against distilled/deionized water through a membrane of nominal cutoff of 3000 Da, and, finally, lyophilized. Purity was checked by mass spectrometry in a Q-TOF (Micromass) and showed the characteristic 4884 Da.

2.2. Muscle contraction experiments

Male Wistar rats weighing 180–200 g were sacrificed in a CO_2 chamber and both soleus and EDL were dissected and transferred to a Petri dish containing regular Krebs–Henseleit solution with the following salts (in mM): NaCl 115, KCl 3.5, $NaHCO_3$ 25, NaH_2PO_4 1, $MgCl_2$ 6, glucose 12, gassed with O_2/CO_2, 95%/5%, and pH = 7.2. Muscles were mounted on isometric transducers of a Powerlab isolated organ system in a 5 mL organ bath with constant gassing. Direct stimulation was performed with a pair of platinum wires running parallel and equally spaced to the muscles, connected to a Grass 88 stimulator delivering square wave pulses of 80 V and 8 ms duration at 0.2 Hz. Data acquisition was performed using the software Chart 4.1 running on an iMac computer. Aliquots of crotamine were added at regular intervals in order to perform a cumulative concentration vs. response curve. Single-dose experiments were performed by adding a single selected amount of toxin to muscles. Two soleus and two EDL muscles were assembled simultaneously and one of each pair was assigned the role of control, to which only vehicle was added at the same time schedules as crotamine to experimental muscles.

2.3. Electrophysiology of $Na_v1.1$–1.6 human sodium channels

Human embryonic kidney 293 (HEK293) cell lines stably expressing human $Na_v1.1$, 1.2, 1.3, 1.5, and 1.6 α-subunits (generously donated by Dr. J.J. Clare of GlaxoSmithKline, Stevenage, UK) were cultured in Dulbecco's modified Eagle's medium supplemented with 10% fetal bovine serum as described in Oliveira et al. (2004). $Na_v1.4$-expressing cells were obtained after transient transfection of a plasmid containing the $hNa_v1.4$ construct (a kind gift from Prof. Diana Conti-Camerino, University of Bari).

The standard extracellular solution contained (in mM): NaCl 70, NMDG 67, $CaCl_2$ 2, $MgCl_2$ 2, HEPES-NaOH 10, and pH = 7.40. The standard pipette solution contained (in mM): K^+-aspartate 130, NaCl 10, $MgCl_2$ 2, EGTA-KOH 10, Hepes-KOH 10, and pH = 7.30 with KOH. When toxin was added to the recording pipette, the solution contained (in mM) CsCl 120, NaCl 20, EGTA 2, HEPES 10, and pH = 7.40. Known quantities of the toxins were dissolved in the extracellular solution immediately before the experiments. When potassium currents were seen, tetrodotoxin (Sigma) was used at 100 nM (on $Na_v1.1$, 1.2, 1.3, 1.4, and 1.6 currents), and the resulting traces were subtracted from control traces to obtain the tetrodotoxin-sensitive currents. The $Na_v1.5$ clone, which has a tetrodotoxin ID_{50} much higher than 100 nM, never showed significant potassium currents at the test potentials. The extracellular solutions were delivered through a 9-hole (0.6-mm) remote-controlled linear positioner with an average response time of 2–3 s that was placed near the cell under study.

Electrophysiological recordings employed the whole-cell voltage-clamp method at room temperature using a MultiClamp 700A (Axon Instruments) as described previously (Faravelli et al., 1996), with pipette resistance of ≅1.5–2.2 MΩ. Cell capacitance and series resistance errors were carefully compensated for (85–90%) before each voltage-clamp protocol was run to reduce the voltage errors to <5% of the protocol pulse. The P/N leak procedure was routinely used. Recordings were usually started 10 min after rupture of the membrane patch to allow intracellular dialysis with the pipette solution.

Voltage-dependent steady-state inactivation was determined by means of a double-pulse protocol in which a conditioning pulse was applied from a holding potential of −80 mV to a range of potentials from −110 to −10 mV in 10 mV increments for 450 ms, immediately followed by a test pulse to −10 mV. The peak current amplitudes during the tests were normalized to the amplitude of the first pulse and plotted against the potential of the conditioning pulse. Voltage-dependent steady-state activation currents were elicited by step depolarization to test potentials ranging from −80 (or −100) to 10 mV from a holding of −120 mV. Peak conductances were calculated and plotted against test potentials. Steady-state activation and inactivation curves were fitted with Boltzmann equations. pClamp 8.2 (Axon Instruments) and Origin 7 (Microcal Inc.) software were routinely used during data acquisition and analysis.

2.4. Sodium currents in neurons of the DRG

DRGs were dissected from newborn Wistar rats. The tissue was minced and treated with trypsin. Neurons and glial cells were dispersed mechanically and plated on polylysine-treated cover glasses. Cells were maintained in culture medium (DMEM, Sigma) supplemented with fetal calf serum (10%) and antibiotics, at 37 °C, in a 5% CO_2 atmosphere. Cells used in the experiments were kept in culture for a period of 1–4 days.

Sodium currents through voltage-activated channels were recorded with the whole-cell configuration of the patch-clamp technique (Hamill et al., 1981). Axopatch 200B amplifier (Axon Instruments) and pClamp software (v. 10, Axon Instruments) were used. Patch microelectrodes had resistances between 2 and 4 MΩ. The composition of intracellular solution was (in mM): NaCl 10, CsF 150, TEA-Cl 10, $MgCl_2$ 4.5, EGTA 9, and HEPES 10, and that of extracellular solution was NaCl 50, Choline-Cl 82, MgCl 1.2, $CaCl_2$ 1.2, $CoCl_2$ 1.0, KCl 4, and HEPES 10. Membrane capacitance was canceled and the access resistance was compensated in 80–90%. Sodium currents were elicited by depolarizing rectangular pulses. Peak current values were quantified for evaluating *I–V* curves, drug effects, stationary activation and inactivation, and recovery from inactivation.

2.5. Behavioral testing

Male Swiss mice weighing 25–30 g were injected i.p. with the toxins crotamine, μ-conotoxin-GIIIa, α- and β-pompilidotoxin, Bc-III, Tx2-6, and tetrodotoxin. Toxins were injected in increasing doses

until a clear behavioral syndrome was observed and allowed description. Most of these toxins were tested in lethal doses but we observed that if the dose is too high, a behavioral syndrome does not have time to develop. Mice were kept in cages for behavioral observation. Three observers annotated patterns of locomotion and general behavior. Special attention was given to the hind-limb paralysis typical of crotamine. Relevant signs were taken on digital video for subsequent evaluations and to document the observations.

2.6. Statistics

Results from the in vitro muscle contraction experiments were analyzed using a four-parameter logistic equation and EC_{50} and Hill slope were calculated using GraphPad Prism software. Confidence intervals (CI_{95}) were used for inferring significance in Hill slope differences. The assay of a single crotamine concentration on muscle contraction was evaluated by a non-parametric Kruskal–Wallis test followed by the Dunn's multiple comparison test.

3. Results

A clear concentration vs. response curve is achieved by adding aliquots of crotamine to the organ bath. As can be observed in Fig. 1, soleus muscle was affected by lower concentrations of toxin, but it demanded higher concentrations of crotamine to be blocked (almost 100 μM), while EDL contractions can be completely abolished by concentrations of about 10 μM. In this kind of experiment, soleus muscle showed a characteristic spontaneous increase in tension as the experiment developed. So our curve was built subtracting this increase as measured in the second muscle run in parallel with the experimental muscle as described above. The same procedure was applied to EDL. With this confounding effect in mind, we designed a second experiment in which the blockade was performed with a single concentration chosen for its best differential effect between the two muscles, as observed in the concentration vs. effect curves (Fig. 1). The chosen concentration was 6.7 μM. Fig. 2 shows again that EDL muscle is more sensitive to crotamine than soleus, confirming the qualitative results of the sigmoidal curves. Soleus muscle contraction was decreased by 14%, while EDL decreased by 57% in this experiment.

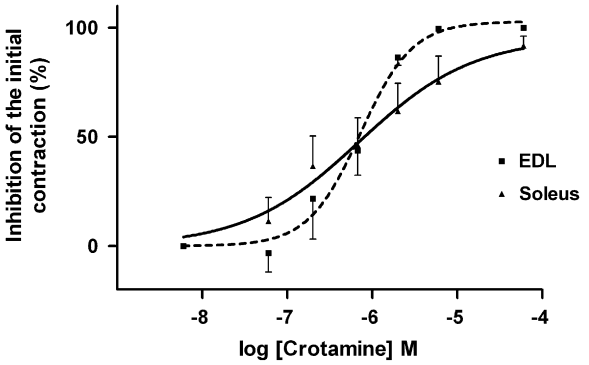

Fig. 1. Cumulative concentration vs. response curves obtained by adding aliquots of crotamine to the incubation bath and recording the direct electrically stimulated contraction of EDL and soleus muscles. Error bars represent SEM. The values of EC_{50} were for EDL 0.72 μM (CI_{95} from 0.45 to 1.16 μM), and for soleus 0.70 μM (CI_{95} from 0.16 to 3.11 μM), Hill slope for EDL 1.42 (CI_{95} from 0.61 to 2.23 μM) and soleus 0.65 (CI_{95} from 0.18 to 1.12 μM), values of R^2 for EDL 0.78 and soleus 0.56.

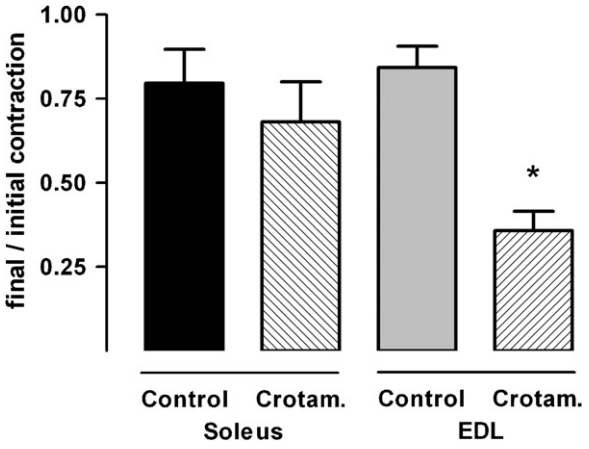

Fig. 2. Effect of a single addition of crotamine (6.7 μM) on soleus and EDL muscle contraction under direct electrical stimulation. Bars represent the mean of 8–10 muscles and error bars represent SEM. *$p \leqslant 0.01$—Kruskal–Wallis followed by Dunn's test.

Although the degree of blockade was different from that observed in the additive sigmoidal curve, it further supports the proposed differential blockade.

Patch-clamp experiments were done on cells expressing the $Na_v1.x$ isoforms of the TTX-sensitive Na^+ channels ($Na_v1.1$–$Na_v1.6$, $n = 3$ for each isoform). Maximal concentrations 1 μM (10 μM for $Na_v1.4$) of crotamine were applied extracellularly for different times (ranging from 2 to 20 min). Crotamine did not affect either the normalized voltage-dependent activation or the steady-state

inactivation, as shown in Fig. 3. Moreover, no change of the peak current density was observed, as shown in Fig. 4E. Data from experiments done specifically on $Na_v1.4$ channels are shown in Fig. 4A and B, where the superimposed traces of the currents elicited at the various test potentials are shown both for activation (A) and inactivation (B) in control and during the extracellular application of 3 μM crotamine (A′ and B′). As a positive control, we also performed an experiment with the *P. nigriventer* spider toxin Tx2-6 (1 μM). This toxin delayed the fast inactivation of sodium channels, as described by others (Matavel et al., 1998), and demonstrated that our system is sufficiently sensitive to detect significant effects, yielding consistent results. Representative traces are presented in

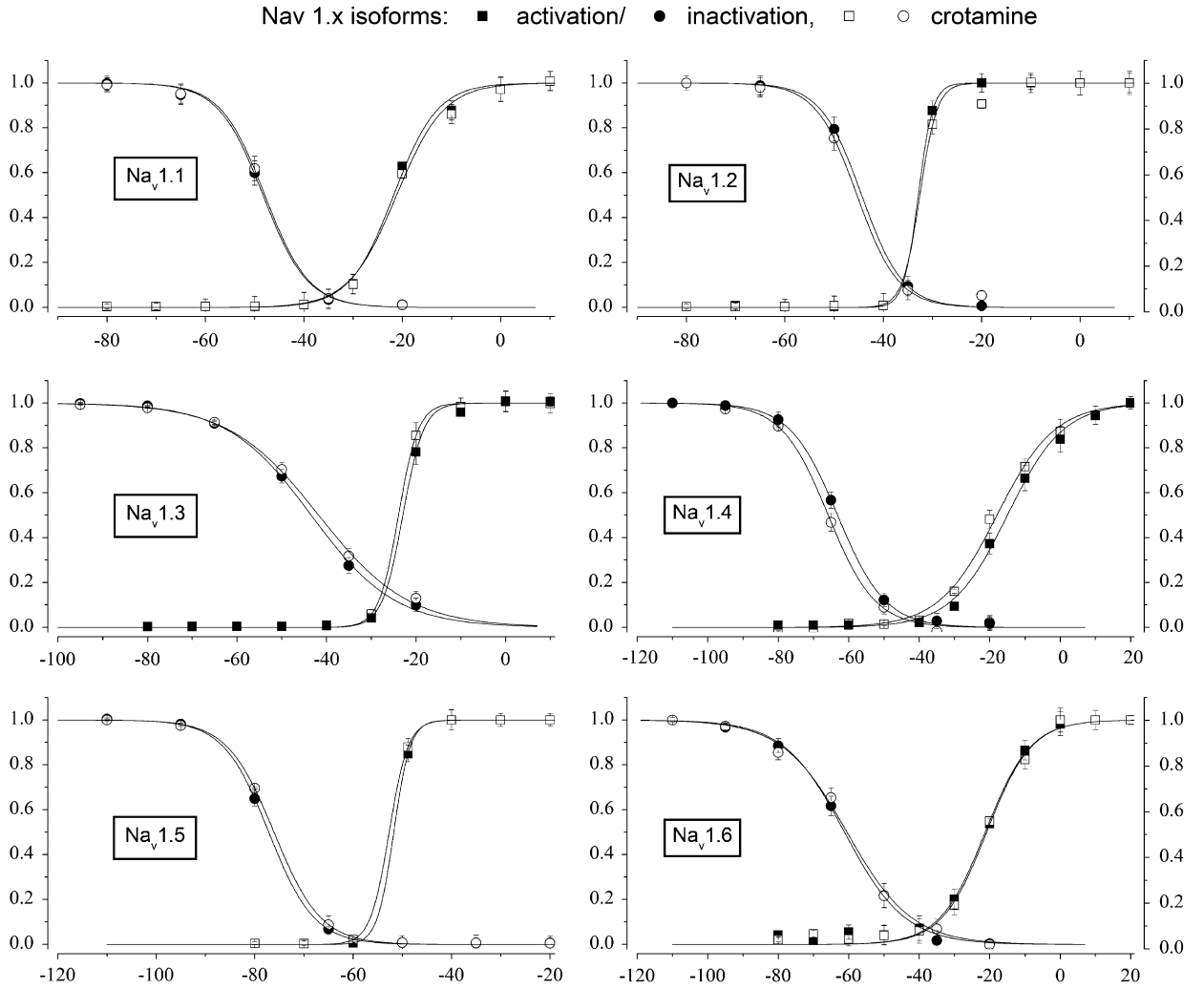

Fig. 3. Steady-state inactivation (rhom) and activation (square) curves for $Na_v1.1$–6 sodium channels in control condition (closed symbols) and after 2 min of extracellular 1 μM crotamine perfusion (open symbols). Experimental data were fitted to a Boltzmann equation, which gave the following $V_{1/2}$ activation, inactivation (V_h), and slope values in control condition and toxin perfusion, respectively (mV): for $Na_v1.1$: $V_{1/2} = -21.76 \pm 0.40$, slope $= 4.44 \pm 0.37$, $V_{1/2} = -21.16 \pm 0.40$, slope $= 4.80 \pm 0.37$; $V_h = -48.30 \pm 0.308$, slope $= -4.51 \pm 0.40$, $V_h = -47.92 \pm 0.29$, slope $= -4.46 \pm 0.36$. $Na_v1.2$: $V_{1/2} = -34.35 \pm 0.26$, slope $= 1.16 \pm 0.069$, $V_{1/2} = -32.56 \pm 1.06$, slope $= 1.73 \pm 0.70$; V_h control and toxin $= -44.38 \pm 0.15$, slope -4.16 ± 0.09. $Na_v1.3$: $V_{1/2} = -23.91 \pm 0.19$, slope $= 2.20 \pm 0.09$, $V_{1/2} = -43.41 \pm 0.37$, slope $= -9.40 \pm 0.33$; V_h control and toxin $= -41.75 \pm 0.47$, slope $= -10.04 \pm 0.42$. $Na_v1.4$: $V_{1/2} = -14.95 \pm 0.4$, slope $= 7.9 \pm 0.4$, $V_{1/2} = -17.95 \pm 0.54$, slope $= 8.2 \pm 0.4$; $V_h = -63.01 \pm 0.21$, slope $= 6.7 \pm 0.20$, $V_h = -65.1 \pm 0.3$, slope $= 6.6 \pm 0.2$. $Na_v1.5$: $V_{1/2} = -52.73 \pm 0.23$, slope $= 1.94 \pm 0.08$, $V_{1/2} = -51.73 \pm 0.13$, slope $= 1.67 \pm 0.07$, $V_h = -77.13 \pm 0.11$, slope $= 4.61 \pm 0.11$, $V_h = -76.08 \pm 0.11$, slope $= 4.77 \pm 0.10$. $Na_v1.6$: $V_{1/2}$ control and toxin $= 20.\ 89 \pm 0.23$, slope $= 6.0 \pm 0.08$, $V_h = -1.18 \pm 0.65$, slope $= 8.59 \pm 0.23$, $V_h = -60.48 \pm 0.12$, slope $= 9.17 \pm 0.43$. Notice the different X scales.

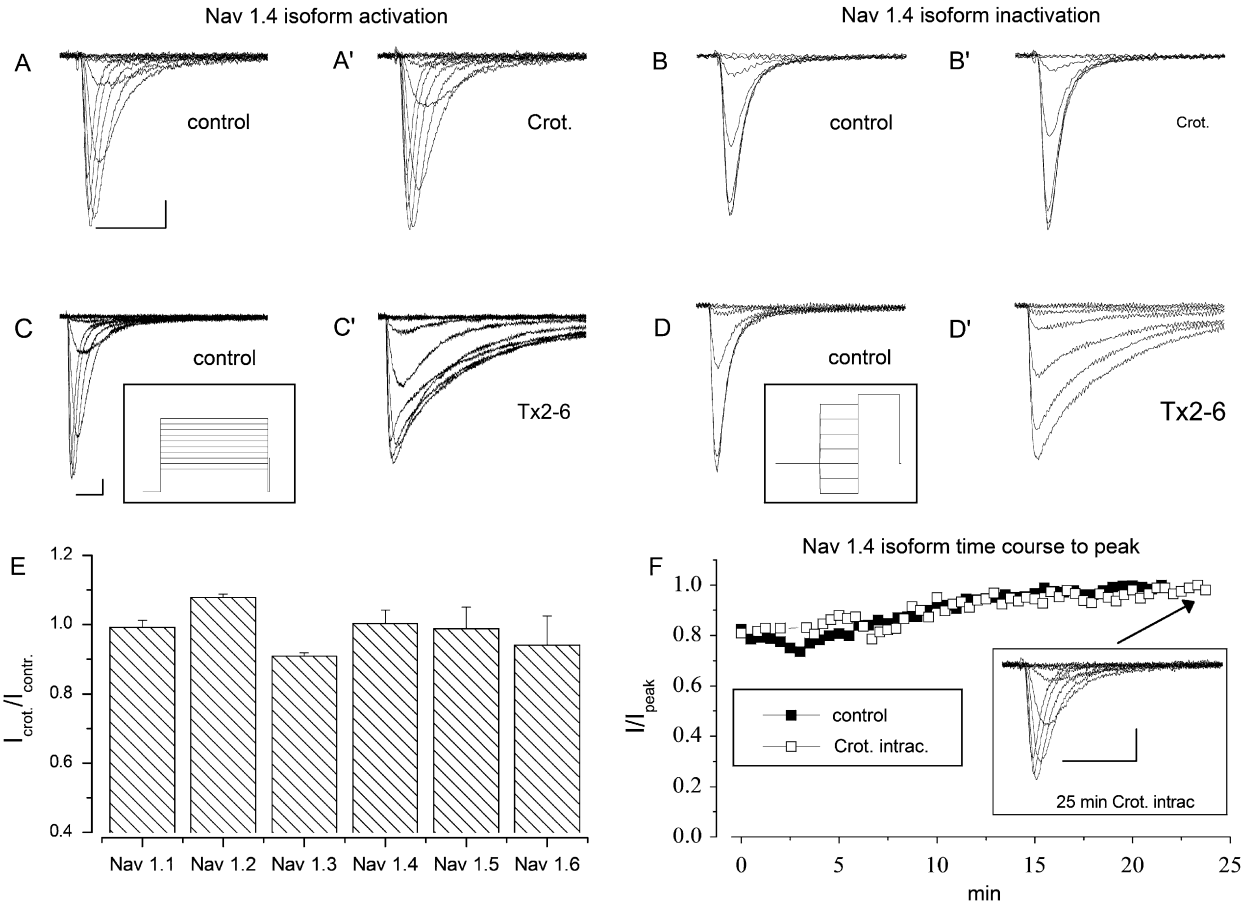

Fig. 4. Current in $Na_v1.4$ channels. (A–D) A family of superimposed currents representing activation (A and C) and inactivation (B and D) of $Na_v1.4$ sodium channel in control condition and after 8 min of 3 μM crotamine extracellular perfusion (A′–B′) or 1 min of 1 μM Tx2-6 extracellular perfusion (C′ and D′). Activation traces are elicited using the protocol shown in the inset to (C). In brief: from a holding potential of −100 mV, a family of depolarizing steps ranging from −80 to +20 mV were applied to activate sodium currents. Inactivation curves are elicited using the protocol shown in the (D) inset. In brief: from a holding potential of −80 mV (−100 mV for $Na_v1.5$) cells are clamped for 180 ms at different depolarizing potential (from −110 to −20 mV) and available currents after conditioning steps are tested at −10 mV. Scale bars: 500 pA, 2 ms. (E) Plot of the ratio of currents recorded (2–10 min) during crotamine perfusion ($I_{crot.}$) with respect to control observed in the different isoforms. Concentrations ranged from 0.5 to 10 μM, $n = 2$–7 for each channel isoform. (F) Plot of normalized peak current in a control cell (closed symbol) and in a cell intracellularly perfused with 0.5 μM crotamine. Current was elicited every 30 s from −100 mV to a test potential of −10 mV. Inset: superimposed currents elicited as in panel (A) at the end of a 25-min-long experiment. Same scales as in panel (A).

Fig. 4C′ and D′. Crotamine was also applied intracellularly in cells expressing $Na_v1.4$ (at a concentration of 0.5 μM for up to 20 min) and the time course of the peak recorded currents is shown in Fig. 4F, demonstrating that the peptide was unable to affect consistently the Na^+ currents.

Fig. 5 shows results of experiments on native sodium currents in the somata of DRG neurons. These cells express mostly $Na_v1.1$, $Na_v1.6$, $Na_v1.8$, and $Na_v1.9$ α subunits. The upper panels show sodium currents elicited by a pulse from −100 to 0 mV, in control and under crotamine conditions. The lower panel shows ratios of peak values of sodium currents (peak current at a time t divided by peak value of the first pulse) in a time series of depolarizing pulses, from −100 to 0 mV, under control and under crotamine. No changes were observed in kinetics or in the peak values of current. Not shown are the results of experiments in which crotamine does not modify stationary activation or inactivation, nor the recovery from inactivation.

The behavioral effects of the sodium channel-acting toxin μ-CgTx-GIIIa at a dose of 7 μg/kg included a flaccid paralysis, so mice were incapable

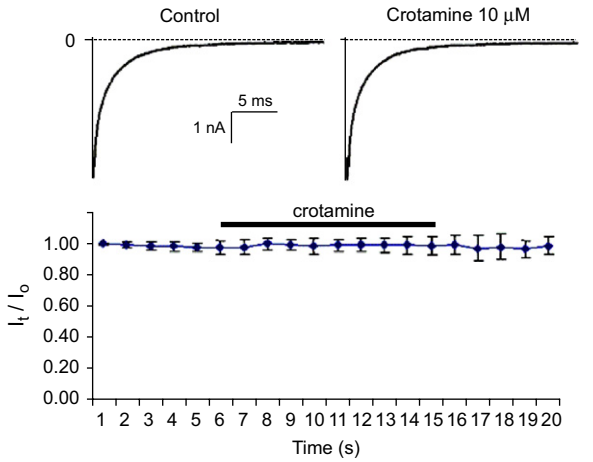

Fig. 5. Sodium currents in the somata of dorsal root ganglia neurons. The upper panels represent currents elicited by pulses to 0 mV, from a holding potential of −100 mV. Crotamine does not modify the kinetics or amplitude of sodium currents. The lower panel shows the ratio of peak values of currents (normalized to the value of the first pulse) in a time series of pulses. No effect of crotamine, in the concentration of 10 µM, is observed.

of sustaining the head or body, micturition, decreased ambulation, and forward movements were accomplished by rapid and synchronic jerks of the four legs, a remarkable exophthalmia was observed; hind paws were kept under the body most of the time and extended backwards only at the very moment of death. The tail was hardened and presented wipe-like movements hardly hitting the ground. The onset of these effects is rather short and lasts for only a few minutes. The animal dies in about 15 min after injection. With the toxin Bc-III at a dose of 600 µg/kg i.p. animals showed signs of intoxication about 15 min after injection. Hypersalivation lead to intense grooming. They were very reactive to touch and possibly hyper-reflexive. Body movements were poorly coordinated, with head bobbing. Animals died in about 15 min after the initial signs of intoxication. α-Pompilidotoxin showed no signs of acute intoxication at doses of 300 µg/kg. β-Pompilidotoxin at a dose of 300 µg/kg showed an immediate reaction suggesting abdominal pain. Mice were restless and moved irregularly and nervously in the home cage, with constant vocalization. Tx2-6 at a dose of 6 µg/kg induced penile erection, salivation, tremors, and pilloerection, in this order. First signs appeared after ca. 60 min and death after 2 h. Penile erection is a peculiar effect of this toxin rarely reported with other toxins (Troncone et al., 1998; Yonamine et al., 2004). Tetrodotoxin at a dose of 10 µg/kg induced behavioral signs similar to those observed with µ-Cgtx-GIIIa, with the tail showing wipe-like movements and synchronized spastic movements of the four legs. Death occurred rapidly, in about 10 min after injection. Crotamine in a dose of 300 µg/kg finally induced the characteristic paralysis of the hind legs. First signs of intoxication appeared after about 20 min. Curiously, the syndrome seemed to be cyclic, with alternating periods of improvement and worsening. During improvement, the animal was capable of walking on the four paws although visibly intoxicated. During worsening, the extended hind legs were present but the animal responded to noxious stimulations to the hind paws; paralysis may also affect front paws, as the fingers remain flexed in a relaxed fist-like position. This worsening may take 1–2 min when a period of fast breathing marks the end of it, then the animal improves and after about 2 min, the crisis is back again. Intoxication follows a progressive fashion until the animal dies. Mice may spend about 30 min in this cyclic worsening until death, apparently by respiratory arrest.

4. Discussion

The present study investigated the hypothesis of a differential susceptibility of slow- and fast-twitching muscles to the action of crotamine, a small basic polypeptide myotoxin obtained from the venom of the snake *C. d. terrificus* in order to explain the characteristic behavioral syndrome of hind-limb paralysis induced by this toxin. Soleus and EDL muscles were employed as slow- and fast-twitching muscles and we observed that, indeed, EDL could be completely paralyzed by lower concentrations of crotamine while soleus demanded higher concentrations of toxin to stop contracting. Cumulative concentration vs. contraction curves (Fig. 1) obtained by direct electrical stimulation in vitro illustrated the differences as well as an experiment in which a selected concentration of crotamine was added in a single application (Fig. 2), showing that an acute effect of crotamine may reflect better the selective action of the toxin. Most of the muscles in the hind limb of mice are fast twitching and only soleus is composed of slow-twitching fibers (Wang and Kernell, 2001a, b). In the experiment with a single concentration of crotamine (Fig. 2), we further demonstrate the appropriateness of our thinking. The blockade obtained by slowly adding

amounts of crotamine to EDL and soleus (Fig. 1) was different. While EDL was blocked almost completely, soleus still retained some contractive capacity. The difference can be attributed to physiological differences between the two muscles (as discussed below) and may point to the true mechanism of action of crotamine, an issue that is reopened by this study. As discussed below, since the mechanism of action of crotamine may involve intracellular sites, we consider that a new concentration vs. response curve made of single doses per muscle would yield different curves from those obtained in additive doses, possibly also revealing different EC_{50}.

Chang and Tseng (1978) have proposed crotamine as a sodium channel toxin after exposing mouse and rat diaphragm to radioactive sodium in the presence of crotamine. They observed an increased accumulation of radioactive sodium in treated muscles compared to control muscles not exposed to crotamine. Later, these authors compared other sodium channel toxins with crotamine and pointed out that this toxin only produced changes after 17 min of exposure (Chang et al., 1983). In the voltage-clamp experiments reported here, no change was observed after 20 min of exposure to a concentration 15 times higher than the used by those authors. Yet, Matavel et al. (1998) observed crotamine-induced increases in the sodium current using a loose patch-clamp in semitendinous frog muscle. Curiously, Chang and Tseng (1978) reported that crotamine was not active on frog muscles. Important issues regarding the purity of crotamine preparations used in these studies may account for these discrepancies. Most of the pharmacological studies on crotamine represent only indirect evidences of the sodium channel activity (Chang et al., 1983; Chang and Tseng, 1978; Matavel et al., 1998). In our study, this question was approached using transfected HEK cells expressing the α subunits of neuronal $Na_v1.1$, $Na_v1.2$, $Na_v1.3$, and $Na_v1.6$, cardiac $Na_v1.5$, and muscle $Na_v1.4$ sodium channels. These cells allow for a direct measure of the effects of crotamine. Surprisingly, no effect was observed on these sodium channels (Figs. 3 and 4). To check for toxin effectiveness, a small aliquot of the same crotamine batch used in patch-clamp experiments was injected in a mouse and the characteristic paralysis was observed. As a second control, a toxin obtained from the *P. nigriventer* spider venom known as Tx2-6 and described as active on site III of the sodium channel (Matavel et al., 2002) was employed. Tx2-6 was effective on $Na_v1.1$ and $Na_v1.4$, as expected, demonstrating that our experiment could reliably detect this kind of effect. Our results support other controversial observations on crotamine published by Fletcher et al. (1996). These authors observed a crotamine-induced reduction in sodium currents measured in patch-clamp experiments using human muscle cell cultures and suggested that the toxin should be internalized to produce its full effects. While internalization was considered unlikely by some authors (Hong and Chang, 1983), it was shown recently that internalization does occur and crotamine may even be found in the nucleus of fibroblasts and lymphoblasts (Kerkis et al., 2004). Considering these observations, we tested whether the toxin can modify sodium currents when applied in the cytoplasmic side of HEK cells by including it in the pipette solution. Again, crotamine was devoid of any effect on these cells expressing $Na_v1.4$ even after 20 min. Since the sodium channels are constituted by other subunits than the α expressed in HEK cells, we decided to examine crotamine's effects on primary cultured DRG neurons. Even then crotamine was devoid of any effect (Fig. 5). Still, although unlikely, we cannot rule out the possibility of an interaction with the β subunit of a muscular sodium channel.

The myonecrotic effects of crotamine and myotoxin-α have been compared and similar vacuolization patterns were found (Cameron and Tu, 1978). Recent studies on myotoxin-α suggested an intracellular site of action involving calcium homeostasis (Baker et al., 1992; Hirata et al., 1999; Mori et al., 1988). Assuming that crotamine is inactive on sodium channels (as demonstrated here) and with myonecrotic activity and molecular structure similar to myotoxin-α, we suggest that both toxins share the same pharmacological profile. Indeed, studies on sarcoplasmic reticulum demonstrated that crotamine could increase intracellular calcium by a ryanodine receptor-mediated process (Fletcher et al., 1996). This would explain why some of the observed effects of crotamine only appear after a certain delay. The toxin should first undergo internalization to induce calcium release from internal stores, then activate metabolic cascades, and only then, possibly, interfere with channel function at a very late stage. This may also lie behind the differences observed in prolonged and acute toxin exposure as the ones depicted in Figs. 1 and 2. Toxins that interfere directly with

sodium channel function would have a faster action.

Our investigation on the behavioral signs of intoxication by crotamine and toxins with proven sodium channel activity further support the notion that crotamine has a different mechanism of action since no other sodium channel toxin mimicked the hind-limb paralysis of crotamine. Tetrodotoxin and μ-conotoxin-GIIIa are blockers of the site I of sodium channels (Li and Tomaselli, 2004) and showed similar behavioral signs. The others (BcIII, Tx2-6, α- and β-pompilidotoxins) are site III sodium channel toxins that delay sodium channel inactivation and again showed related behaviors. Crotamine should have behavioral effects similar to the latter toxins, but this was not the case since hind-limb paralysis was not observed with the other toxins and crotamine did not induce hypersalivation, priapism, and the other signs observed with the site III toxins.

In conclusion, this investigation showed that crotamine (a) does not interfere directly with sodium channel function; (b) slow- and fast-twitching muscles are differentially affected by crotamine; (c) the resemblance between crotamine and myotoxin-α regarding structure and also some few pharmacological characteristics suggest that these toxins have the same pharmacological target; and (d) an appropriate description of their mechanism of action is still lacking.

Acknowledgments

We would like to thank Dr. J.J. Clare for permitting the use of GlaxoSmithKline $Na_v1.x$ cell clones. This study was partially supported by grants from the Italian Ministero dell'Università e della Ricerca Scientifica e Tecnologica (2003052919, MIUR-FIRB2001-RBNE01XMP4-002, MIUR-FISR2001 0300179), the Università di Milano-Bicocca to EW. ES is a Ph.D. student of Physiology at the Department of Biotechnologies and Biosciences of the University of Milano-Bicocca. We also thank Dr. K. Konno (Butantan) for kindly supplying pompilidotoxins.

References

Baker, B., Utaisincharoen, P., Tu, A.T., 1992. Structure–function relationship of myotoxin a using peptide fragments. Arch. Biochem. Biophys. 298 (2), 325–331.

Beltran, J.R., Mascarenhas, Y.P., Craievich, A.F., Laure, C.J., 1985. Saxs study of structure and conformational changes of crotamine. Biophys. J. 47 (1), 33–35.

Beltran, J.R., Mascarenhas, Y.P., Craievich, A.F., Laure, C.J., 1990. SAXS study of the snake toxin alpha-crotamine. Eur. Biophys. J. 17 (6), 325–329.

Bewick, G.S., Reid, B., Jawaid, S., Hatcher, T., Shanley, L., 2004. Postnatal emergence of mature release properties in terminals of rat fast- and slow-twitch muscles. Eur. J. Neurosci. 19 (11), 2967–2976.

Boni-Mitake, M., Costa, H., Spencer, P.J., Vassilieff, V.S., Rogero, J.R., 2001. Effects of (60)Co gamma radiation on crotamine. Braz. J. Med. Biol. Res. 34 (12), 1531–1538.

Cameron, D.L., Tu, A.T., 1978. Chemical and functional homology of myotoxin a from prairie rattlesnake venom and crotamine from South American rattlesnake venom. Biochim. Biophys. Acta 532 (1), 147–154.

Chang, C.C., Tseng, K.H., 1978. Effect of crotamine, a toxin of South American rattlesnake venom, on the sodium channel of murine skeletal muscle. Br. J. Pharmacol. 63 (3), 551–559.

Chang, C.C., Hong, S.J., Su, M.J., 1983. A study on the membrane depolarization of skeletal muscles caused by a scorpion toxin, sea anemone toxin II and crotamine and the interaction between toxins. Br. J. Pharmacol. 79 (3), 673–680.

Cheymol, J., Goncalves, J.M., Bourillet, F., Roch-Arveiller, M., 1971. A comparison of the neuromuscular action of crotamine and the venom of *Crotalus durissus terrificus* var. *crotaminicus*. 1. Neuromuscular preparations in situ. Toxicon 9 (3), 279–286.

Endo, T., Oya, M., Ozawa, H., Kawano, Y., Giglio, J.R., Miyazawa, T., 1989. A proton nuclear magnetic resonance study on the solution structure of crotamine. J. Protein Chem. 8 (6), 807–815.

Faravelli, L., Arcangeli, A., Olivotto, M., Wanke, E., 1996. A HERG-like K+ channel in rat F-11 DRG cell line: pharmacological identification and biophysical characterization. J. Physiol. 496 (Pt 1), 13–23.

Fletcher, J.E., Hubert, M., Wieland, S.J., Gong, Q.H., Jiang, M.S., 1996. Similarities and differences in mechanisms of cardiotoxins, melittin and other myotoxins. Toxicon 34 (11–12), 1301–1311.

Hamill, O.P., Marty, A., Neher, E., Sakmann, B., Sigworth, F.J., 1981. Improved patch-clamp techniques for high-resolution current recording from cells and cell-free membrane patches. Pflug. Arch. 391 (2), 85–100.

Hampe, O.G., Vozari-Hampe, M.M., Goncalves, J.M., 1978. Crotamine conformation: effect of pH and temperature. Toxicon 16 (5), 453–460.

Hirata, Y., Nakahata, N., Ohkura, M., Ohizumi, Y., 1999. Identification of 30 kDa protein for Ca(2+) releasing action of myotoxin a with a mechanism common to DIDS in skeletal muscle sarcoplasmic reticulum. Biochim. Biophys. Acta 1451 (1), 132–140.

Hong, S.J., Chang, C.C., 1983. Potentiation by crotamine of the depolarizing effects of batrachotoxin, protoveratrine A and grayanotoxin I on the rat diaphragm. Toxicon 21 (4), 503–514.

Kerkis, A., Kerkis, I., Radis-Baptista, G., Oliveira, E.B., Vianna-Morgante, A.M., Pereira, L.V., Yamane, T., 2004. Crotamine is a novel cell-penetrating protein from the venom of rattlesnake *Crotalus durissus terrificus*. FASEB J. 18 (12), 1407–1409.

Laure, C.J., 1975. The primary structure of crotamine (author's translation). Hoppe Seylers Z. Physiol. Chem. 356 (2), 213–215.

Li, R.A., Tomaselli, G.F., 2004. Using the deadly mu-conotoxins as probes of voltage-gated sodium channels. Toxicon 44 (2), 117–122.

Matavel, A.C., Ferreira-Alves, D.L., Beirao, P.S., Cruz, J.S., 1998. Tension generation and increase in voltage-activated Na + current by crotamine. Eur. J. Pharmacol. 348 (2–3), 167–173.

Matavel, A., Cruz, J.S., Penaforte, C.L., Araujo, D.A., Kalapothakis, E., Prado, V.F., Diniz, C.R., Cordeiro, M.N., Beirao, P.S., 2002. Electrophysiological characterization and molecular identification of the *Phoneutria nigriventer* peptide toxin PnTx2-6. FEBS Lett. 523 (1–3), 219–223.

Mori, N., Tu, A.T., Maurer, A., 1988. Characterization of nicked myotoxin a and its effect on the sarcoplasmic reticulum calcium pump. Arch. Biochem. Biophys. 266 (1), 171–180.

Nicastro, G., Franzoni, L., de Chiara, C., Mancin, A.C., Giglio, J.R., Spisni, A., 2003. Solution structure of crotamine, a Na + channel affecting toxin from *Crotalus durissus terrificus* venom. Eur. J. Biochem. 270 (9), 1969–1979.

Oliveira, J.S., Redaelli, E., Zaharenko, A.J., Cassulini, R.R., Konno, K., Pimenta, D.C., Freitas, J.C., Clare, J.J., Wanke, E., 2004. Binding specificity of sea anemone toxins to Nav 1.1–1.6 sodium channels: unexpected contributions from differences in the IV/S3–S4 outer loop. J. Biol. Chem. 279 (32), 33323–33335.

Teno, A.M., Vieira, C.A., Santoro, M.M., Neves, A.G., Giglio, J.R., 1990. Interchain disulfide bonds in crotamine self-association. J. Biochem. (Tokyo) 107 (6), 821–825.

Troncone, L.R.P., Lebrun, I., Hipolide, D.C., Raymond, R.R., Nobrega, J.N., 1998. Regional brain c-Fos activation associated with penile erection and other symptoms by the spider toxin TX2-6. Naunyn-Schmiedebergs Arch. Pharmacol. 358 (1 (Suppl. 1)), R38.

Wang, L.C., Kernell, D., 2001a. Fibre type regionalisation in lower hindlimb muscles of rabbit, rat and mouse: a comparative study. J. Anat. 199 (Pt 6), 631–643.

Wang, L.C., Kernell, D., 2001b. Quantification of fibre type regionalisation: an analysis of lower hindlimb muscles in the rat. J. Anat. 198 (Pt. 3), 295–308.

Yonamine, C.M., Troncone, L.R.P., Camillo, M.A.P., 2004. Blockade of neuronal nitric oxide synthase abolishes the toxic effects of Tx2-5, a lethal *Phoneutria nigriventer* spider toxin. Toxicon 44 (2), 169–172.